Neural Network for Odor Sensor Array Spike Encoding Inspired by Mammalian Olfaction

Hantao Li
the School of Microelectronic and Communication Engineering
Chongqing University
Chongqing, China
hantaoli@cqu.edu.cn

Fengchun Tian*
the School of Microelectronic and Communication Engineering
Chongqing University
Chongqing, China
fengchuntian@cqu.edu.cn

Siyuan Deng
the School of Microelectronic and Communication Engineering
Chongqing University
Chongqing, China
20183669@cqu.edu.cn

Leilei Zhao
the School of Microelectronic and Communication Engineering
Chongqing University
Chongqing, China
leileizhao@cqu.edu.cn

Zhiyuan Wu
the School of Microelectronic and Communication Engineering
Chongqing University
Chongqing, China
wuzhiyuan@cqu.edu.cn

Yue Liu
the School of Microelectronic and Communication Engineering
Chongqing University
Chongqing, China
liuyue@stu.cqu.edu.cn

2023 8th International Conference on Communication, Image and Signal Processing (CCISP) | 979-8-3503-0583-8/23/$31.00 ©2023 IEEE | DOI: 10.1109/CCISP59915.2023.10355792

***Abstract*—Signal processing in electronic nose (e-nose) odor detection involves a series of complex and time-consuming steps, such as noise reduction, filtering, normalization in signal preprocessing, as well as feature generation, selection, and dimensionality reduction. When dealing with different gas sensors, these processing methods might require meticulous adjustments, and each sensor might need own specific processing strategy. Such strategies are often tedious and overly reliant on intricate feature engineering, leading to time-consuming operations and poor reproducibility. To address this issue, this paper proposes a biomimetic olfactory perception model inspired by the mammalian olfactory system. Unlike traditional e-nose methods, our model deeply simulates the core structures and functions of the mammalian olfactory system, especially the biomimetic design for neural conduction and information encoding. This allows the model to directly handle the raw sensor responses of the e-nose, eliminating the conventional preprocessing and feature selection steps. The experimental results show that our biomimetic model achieved an average recognition rate of 95.8% on a traditional Chinese medicine dataset, significantly outperforming the traditional method's 90.84%. The model not only demonstrates excellent feature extraction capabilities but also shows extreme robustness when the types and numbers of sensors change, enhancing the reliability and accuracy of the electronic nose in practical applications.**

Keywords—sensor array, digital signal processing, spike encoding, neural network, olfactory model

I. INTRODUCTION

With the continuous advancement of technology, simulating and extending the perceptual capabilities of biological systems has become a popular research direction [1]. Olfaction, as one of the five senses, are closely connected to our daily lives and various industrial fields, such as medicine, food, and environmental monitoring [2]. To more effectively capture and analyze odors, the technology of electronic noses emerged in the 1980s [3]. Distinct from traditional gas analysis instruments, electronic noses (e-noses) aim to mimic the olfactory process of biological noses. They identify complex odors by integrating various sensors and algorithms [4]. Benefiting from the biological olfactory system, e-noses have achieved significant results in many fields, such as food safety and medical diagnosis [5]-[7]. However, they still face numerous challenges. For instance, the data processing procedure relies on intricate and tedious feature engineering and preprocessing steps, which not only increase the operation complexity but also affect its reproducibility [8]. Simultaneously, its accuracy is often impacted due to disturbances from external factors such as sensor drift and environmental changes [9]. To address these issues, a profound study of the mechanisms of olfactory neural networks provides direction for the optimization of e-noses.

The biological olfactory system, through millions of years of evolution, has formed an efficient and robust odor recognition mechanism that can stably identify odors even with changes in concentration [10]. The biological olfactory system translates odor stimuli into spatiotemporal neural activities, regardless of concentration changes [11]. The mammalian olfactory system, including olfactory receptors, the olfactory bulb, and others, has the olfactory bulb as the core information processing part. Various models have researched its mechanism, such as the olfactory bulb model by Li and Cleland [12], the mammalian olfactory bulb model by Viertel [13], and the mathematical model by Kersen [14]. Inspired by the biological olfactory system, researchers are improving data processing techniques for electronic noses. Using biomimetic olfactory models, electronic noses possess high sensitivity, powerful noise reduction capabilities, and resistance to sensor drift, enabling them to accurately identify and estimate odor concentrations. For example, Hyusim and others simulated olfactory receptor neurons, while other researchers used high-density electrochemical sensors to form large sensor arrays [15].

This work was supported by the National Natural Science Foundation of China (No. 62171066)

However, the application of these models may have certain limitations, such as sensor types and computational burdens. Recent research suggests that converting sensor signals into spike patterns can more authentically simulate the mammalian olfactory system. This time coding helps enhance olfactory perception while requiring fewer neurons for rapid signal processing [16]. For instance, Sarkar and Bhonderkar proposed a new encoding strategy [17], and Wang and others encoded within sensor responses, achieving good classification [18]. Although spike encoding is effective, most methods have not considered the temporal characteristics of sensor data. Some studies have successfully employed spiking neural networks to develop biologically-based recognition methods. For example, Vanarse and others constructed classifiers for neuromorphic hardware devices, achieving efficient gas signal encoding and classification [19]. Additionally, inspired by the mammalian olfactory system, Borthakur and Cleland developed a biomimetic algorithm for online learning and drift resistance [20].

In our research, inspired by the mammalian olfactory system, we specifically designed a biomimetic olfactory neural network to optimize data processing for the e-nose. Unlike traditional approaches, our model features particular structural adjustments, emphasizing the mechanisms of convergence and lateral inhibition, making it closer to biological olfactory processing. Notably, we integrated the olfactory epithelium and olfactory bulb layers from the biological olfactory system with e-nose data processing. The biomimicry of these two layers played a pivotal role in handling the response signals from gas sensors. Converting sensor data into spike time sequences not only simplified the data processing procedure but also significantly enhanced the efficiency and accuracy of feature extraction and classification from e-nose data. The following is a summary of the contributions of biomimetic network.

- The model simulates the mammalian olfactory signal transduction process, which automatically learns spatiotemporal information in spike sequences and automates feature extraction, eliminating the need for manual operation based on experience. This greatly simplifies the traditional information processing process of e-nose, eliminating tedious signal preprocessing, feature extraction, selection, and reconstruction steps, while avoiding the deterioration of subsequent pattern recognition algorithm performance due to manual operation failure.
- The model utilizes spiking encoding to transform sensor responses into a more suitable computational model of models, enhancing its biological plausibility. By refining and integrating olfactory information within spike sequences, the model generates latent discriminative features, improving classification performance and robustness of the e-nose system.

The remainder of this paper is organized as follows: Section 2 introduces the basic structure of the proposed olfactory neural network. Section 3 presents the design of the e-nose and the collection of experimental data. Section 4 compares the experimental results and performance analysis of different methods. Finally, conclusions are drawn in Section 5.

II. Basic Structure of the Olfactory Neural Network

A. Biomimetic Olfactory Epithelium

This section simulates the biological olfactory epithelium, mainly responsible for receiving data from the sensor array and converting this data into pulse sequences through specific encoding strategies. For this purpose, we employed a method based on channel coding.

Firstly, for the response value of the i-th sensor, we defined a dynamic range adjuster $\mathcal{R}_i(t)$, which aims to ensure that the data we handle is within a standardized range. It can be represented by the following equation:

$$\mathcal{R}_i(t) = \frac{V_i(t) - \min(V_i)}{\max(V_i) - \min(V_i)} \tag{1}$$

Where $\mathcal{R}_i(t)$ is the normalized value for the i-th sensor at time t, and $V_i(t)$ is the response value of the i-th sensor at time t.

Next, we utilize a Gaussian activation function to define the virtual receptive field $\mathcal{G}_k(t)$. This approach allows us to accurately capture and encode the responses of the sensors. Each virtual receptor's receptive field should cover the entire time range of the sensor's response $[t_{min}, t_{max}]$. The definition of the virtual receptive field is as follows:

$$\begin{cases} \mathcal{G}_k(t) = \exp\left[-\dfrac{(t-\mu_k)^2}{2\sigma_k^2}\right] \\ \mu_k = t_{min} + \left[\dfrac{(2k-3)(t_{max}-t_{min})}{2(n-2)}\right] \\ \sigma_k = \dfrac{t_{max}-t_{min}}{\lambda(n-2)} \end{cases} \tag{2}$$

Where μ_k and σ_k are the center and width of the Gaussian function, respectively, n is the number of virtual receptive fields, and λ is an adjustment parameter used to modulate the distribution of receptive fields, with a specific value of 1.5 [21].

To generate spike timings, we focus on the intersections of the sensor response with each virtual receptive field. The timings of these intersections can be obtained using the following equation:

$$\mathcal{T}_{ik} = \{t | \mathcal{R}_i(t) = \mathcal{G}_k(t),\ t_{min} < t < t_{max}\} \tag{3}$$

Moreover, to capture the most meaningful information[22], we only consider the first intersection of the sensor response with each receptive field as the spike timing:

$$\mathcal{S}_T = \{\mathcal{T}_{ik}(0), 1 \le i \le m, 1 \le k \le n\} \tag{4}$$

Where n is the number of virtual receptive fields and m is the number of sensors.

Through the aforementioned method, we not only retain the original characteristics of the sensors but also provide a robust encoding mechanism that can accurately perform odor recognition in the biomimetic olfactory network.

B. Biomimetic Olfactory Bulb Layer

We constructed a biomimetic neural network to simulate the mammalian olfactory system, refining odor information from spike timings in a biological manner. The basic structure is shown in Fig. 1. This section simulates the biological olfactory bulb layer, receiving pulse signals from the olfactory epithelium layer. The model comprises five types of neurons: Mitral Cells (MC), Granule Cells (GC), External Tufted Cells (ET), Periglomerular Cells (PG), and Short-Axon Cells (SA), where '+' and '−' represent excitatory and inhibitory synapses, respectively.

We chose the LIF (Leaky Integrate-and-Fire) model to describe neuron activity, with the neuron model described as follows:

$$\tau_m \frac{du}{dt} = -u(t) + RI(t) \tag{5}$$

Where $\tau_m = RC$ represents the membrane time constant, which determines the rate of change of the neuron potential. $u(t)$ represents the membrane potential of the neuron, R represents the membrane resistance, and $I(t)$ is the total current flowing into the neuron, which can include synaptic input, injected current, or current from other sources.

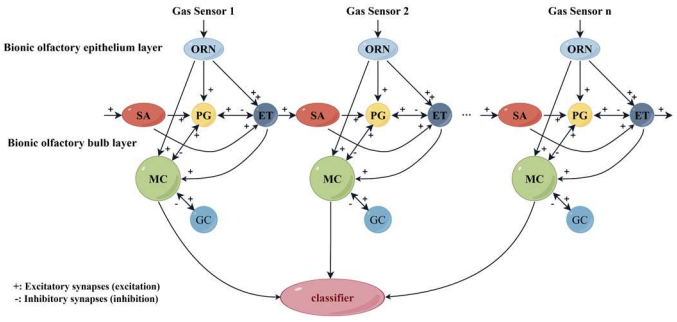

FIG. 1: BASIC STRUCTURE OF THE BIOMIMETIC OLFACTORY NEURAL NETWORK

When the membrane potential $u(t)$ reaches or exceeds the threshold V_{th}, the neuron fires an action potential, and the membrane potential is immediately reset to V_{reset}.

In this model, the MC (Mitral Cells) are the core part of information processing, responsible for transmitting and initially processing the information. GC (Granule Cells) modulate odor information, ET (External Tufted Cells) participate in discerning the concentration of odors, while SA (Short-Axon Cells) and PG (Periglomerular Cells) enhance communication between neurons, ensuring the accuracy of odor recognition. Biomimetic olfactory receptors (ORN) convey pulses to MCs, ETs, and PGs through excitatory synapses. Particularly, the connection between MC and GC is pivotal in odor recognition.

We selected parameters for different neurons and, through experimental iteration, found the optimal values for these parameters, as shown in Table 1.

To simulate synaptic plasticity in the neural system, we adopted Spike Timing Dependent Plasticity (STDP) as the synaptic learning rule [23]. This adjusts synaptic weights based on the time difference between pre-synaptic and post-synaptic neuron spikes. Using this approach, our model can adaptively adjust its weights, allowing the neuron population to better respond to the inputs they receive, making the behavior of the biomimetic model closer to that of a real neural system.

TABLE 1: LIF MODEL PARAMETERS FOR DIFFERENT NEURON TYPES IN THE BIOMIMETIC OLFACTORY NEURAL NETWORK

Parameters	MC	PG	GC	ET	SA
τ_m	2.5	2.5	2.5	2.5	2.5
R	1	1	1	1	1
V_{rest}	0	0	0	0	0
V_{th}	10	10	15	15	15
V_{reset}	-5	-5	-5	-5	-5
T_{ref}	2.5	2.5	2.5	2.5	2.5

In the olfactory neural network model we constructed, the oscillation curve of the dynamic changes in the mitral cell membrane potential serves as the output of the olfactory neural network. This dynamic membrane potential change curve reveals the central role of neural oscillations in information processing. To extract key features from these dynamic changes, we computed the variance of the membrane potential changes of all mitral cells and used it as input for the classifier. This variance-based feature extraction method is more concise than traditional methods while ensuring high accuracy.

Although the olfactory neural network can effectively capture the main features of odors, due to the lack of a feedback mechanism in the model, we still employed traditional pattern recognition techniques, such as Linear Discriminant Analysis (LDA), Support Vector Machines (SVM), Random Forests (RF), Extreme Learning Machine (ELM), and Back Propagation Artificial Neural Network (BP-ANN) for classification. To precisely evaluate the performance of each classification method, we adopted the five-fold cross-validation method, ensuring that each sample was assessed as validation data.

III. DESIGN OF THE ELECTRONIC NOSE AND EXPERIMENTAL DATA COLLECTION

A. E-Nose System

We designed and constructed a sensor array containing 41 commercial gas sensors, including 37 gas-sensitive sensors and 4 environmental monitoring sensors. Details of each sensor can be found in reference [9]. The basic structure, as shown in Fig. 2, reveals its composition, including detection units, sampling units, and control units. All sensors are fixed on a Printed Circuit Board (PCB) and connected to the pins of their respective packages.

The dataset collected in this study covers five traditional Chinese medicines: Honeysuckle (Jin Yin Hua), Coptis (Huang Lian), Anemarrhena (Zhi Mu), Mugwort (Ai Ye), and Patchouli (Guang Huo Xiang). For each experiment (i.e., each sample), 1 gram of the sample was taken, with 30 experiments conducted for each type of traditional medicine, resulting in a total of 150 sets of data. The sample collection process was strictly in accordance with laboratory standard operating procedures, ensuring the consistency and reliability of the data. All samples underwent the same preprocessing steps to minimize potential errors. Their specific names and features are listed in Table 2. To obtain the volatile compounds of these traditional Chinese medicines, we sealed the samples in specimen bottles and let

them sit for 8 hours until the concentration reached saturation. This time setting ensures the release of most volatile compounds.

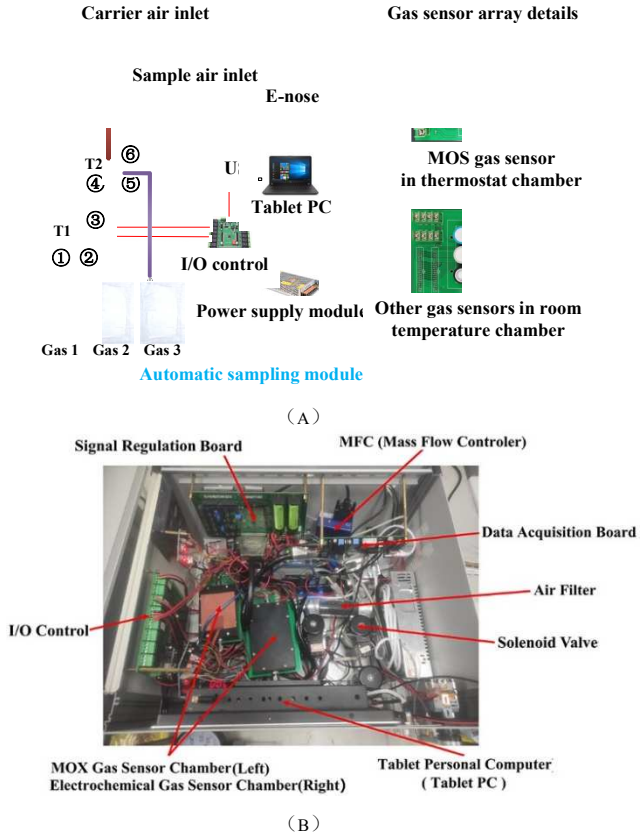

FIG. 2: BASIC STRUCTURE OF THE ELECTRONIC NOSE. (A) SYSTEM FRAMEWORK OF THE ELECTRONIC NOSE; (B) HARDWARE COMPONENTS OF THE ELECTRONIC NOSE.

TABLE 2: INFORMATION TABLE FOR TRADITIONAL CHINESE MEDICINE SAMPLES

Medicine Name	Origin	Processing Method	Quality	Sample Count
Honeysuckle (Jin Yin Hua)	Shandong	Dried by baking	Second Grade	30
Coptis (Huang Lian)	Hebei	Chopped and sun-dried	Second Grade	30
Anemarrhena (Zhi Mu)	Hebei	Sliced and sun-dried	Third Grade	30
Mugwort (Ai Ye)	Sichuan	Chopped and sun-dried	Standard	30
Patchouli (Guang Huo Xiang)	Guangxi	Sliced and sun-dried	Standard	30

To ensure the accuracy of the experiment, all pipelines and sensing chambers were cleaned before each measurement to ensure that the volatile compounds of the traditional Chinese medicines did not remain on the sensors and pipelines. We cleaned the sensor chamber and pipelines with pure air for 15 minutes. After that, the sensors could return to baseline levels. The sampling process followed the steps below:

(1) Baseline Phase (P1): The system was injected with zero-grade air for 2 minutes, with a flow rate of 500mL/min and a temperature of 30°C, to detect the baseline of the sensors.

(2) Post-Baseline Phase (P2): Serving as a buffer, this phase lasted for 1 minute with a flow rate of 40mL/min and a temperature of 30°C, ensuring the accuracy of the baseline response.

(3) Sample Introduction Phase (P3): The test gas was automatically injected into the sensor chamber with a flow rate of 40mL/min and a temperature of 30°C, lasting for 6 minutes.

(4) Sensor Cleaning Phase (P4): The sensors were cleaned using pure air with a flow rate of 500mL/min, at a temperature of 30°C, lasting for 15 minutes.

The total experiment duration was 24 minutes, with a sampling rate of 1Hz. The gas flow rate was 40ml/min for the P2 and P3 phases, and 500ml/min for the P1 and P4 phases. Before the start of the experiment, the sensors were pre-heated for 7 days to ensure the consistency of the response patterns for each measurement.

B. Data processing methods

In this study, we directly fed the raw response curves of the gas sensors into the olfactory neural network, without any prior data preprocessing. The neural network produced membrane potential change curves for the mitral cells corresponding to the number of sensors. Different membrane potential change curves demonstrated the unique output characteristics of the biomimetic olfactory perception network for different input odors, as shown in Fig. 3.

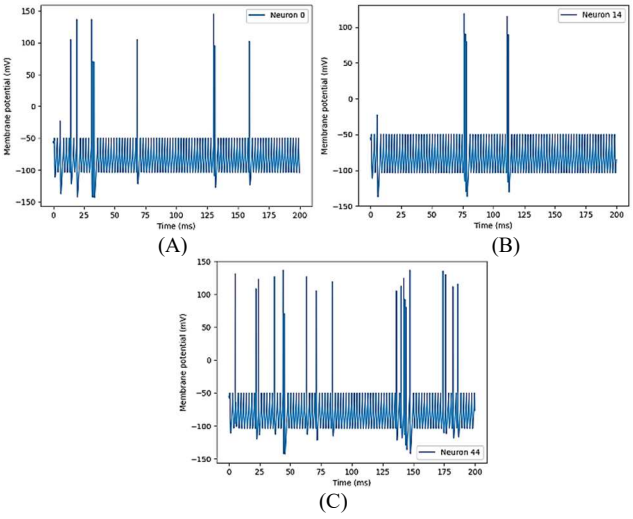

FIG. 3: OUTPUT CURVES OF DIFFERENT MITRAL CELLS. (A) MITRAL CELL 1; (B) MITRAL CELL 14; (C) MITRAL CELL 44.

To more intuitively display the characteristics of the network output, Fig. 3 provides a detailed display of the outputs of three mitral cells. The variance is calculated from the output of each mitral cell, with the output divided into n=18 segments, aiding in the derivation of oscillation strength information. Then, the segmented variances of all mitral cells are used as features extracted by the biomimetic network, which are fed into subsequent classifiers for odor recognition. To better test

the performance of the olfactory neural network, five traditional classification methods were used: Linear Discriminant Analysis (LDA), Support Vector Machine (SVM), Random Forest (RF), Extreme Learning Machine (ELM), and Backpropagation Artificial Neural Network (BP-ANN).

In addition, traditional data processing methods were used for comparison. The traditional data processing of the electronic nose covers steps such as data preprocessing, feature selection, and dimensionality reduction. We employed four data preprocessing methods to mitigate the influence of noise and compensate for drift. Based on the response curves of the sensors, eight features were selected, and a method based on mutual information was used for feature selection [24].

IV. Experiments and Discussions

After the text edit has been completed, the paper is ready for the template. Duplicate the template file by using the Save As command, and use the naming convention prescribed by your conference for the name of your paper. In this newly created file, highlight all of the contents and import your prepared text file. You are now ready to style your paper; use the scroll down window on the left of the MS Word Formatting toolbar.

To evaluate predictive ability, we employed a five-fold cross-validation method. We compared the performance of the traditional data processing method with the newly proposed olfactory neural network on the traditional Chinese medicine dataset. The results show that our proposed model significantly outperforms the traditional methods in terms of classification accuracy. Based on the new olfactory neural network, the highest classification rate reached 98.1%, while the traditional method peaked at 95.3%. Moreover, our biomimetic model achieved an average recognition rate of 95.8% on the traditional Chinese medicine dataset, clearly surpassing the traditional method's 90.84%, as shown in Table 3.

TABLE 3: COMPARISON OF THE BIOMIMETIC MODEL AND TRADITIONAL METHODS

Classifier	Olfactory Neural Network	Traditional Method
LDA	90.8%	94.4%
SVM	97.0%	92%
RF	96.1%	90.5%
ELM	98.1%	82%
BP-ANN	97.0%	95.3%
Avg	**95.8%**	90.84%

Additionally, this model not only demonstrated superior feature extraction capabilities but also exhibited strong robustness when the types and numbers of sensors varied, as can be seen in Fig. 4. As the number of sensors in the array decreased, the model still managed to maintain a good odor recognition ability. Even when only 7 sensors remained in the array, the model's recognition rate still reached 88.2%.

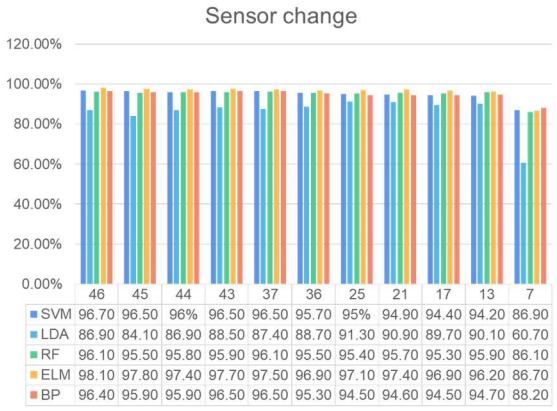

FIG. 4. MODEL RECOGNITION RATE FLUCTUATIONS DUE TO CHANGES IN THE NUMBER OF SENSORS.

Furthermore, the new olfactory neural network not only improved classification accuracy but also greatly streamlined the data processing of the e-nose, making the classification and prediction of different types of traditional Chinese medicine more intuitive and concise.

V. Conclusion

In this study, we proposed a biomimetic network framework aimed at enhancing the data processing of electronic noses and increasing their accuracy in identifying traditional Chinese medicine. Inspired by the mammalian olfactory system, we successfully transformed sensor data into a spike pattern and directly used the raw response curves of the gas sensors as network inputs. Its main advantage lies in its unique coding strategy, allowing for thorough extraction of information from sensor responses. The temporally and spatially rich spike sequences produced by the biomimetic olfactory epithelium layer provide a more accurate signal basis for subsequent classification. Compared with traditional methods, this approach significantly simplifies the data processing flow, enhances the overall processing efficiency, and avoids complex preprocessing and feature selection steps.

Experimental results indicate that the olfactory neural network achieves an average classification recognition rate of 95.8% on the traditional Chinese medicine dataset, significantly outperforming the traditional method's 90.84%. This not only validates the superior feature extraction capability of our proposed model but also demonstrates its robustness to variations in sensor type and count, enhancing the reliability and accuracy of the electronic nose in practical applications.

References

[1] Full J, Baumgarten Y, Delbrück L, et al. Market perspectives and future fields of application of odor detection biosensors within the biological transformation—A systematic analysis[J]. Biosensors, 2021, 11(3): 93.

[2] Farnum A, Parnas M, Apu E H, et al. Harnessing insect olfactory neural circuits for detecting and discriminating human cancers[J]. Biosensors and Bioelectronics, 2023, 219: 114814.

[3] Persaud K, Dodd G. Analysis of discrimination mechanisms in the mammalian olfactory system using a model nose[J]. Nature, 1982, 299(5881): 352-355.

[4] Lledo P M, Gheusi G, Vincent J D. Information processing in the mammalian olfactory system[J]. Physiological reviews, 2005, 85(1): 281-317.

[5] Xing Z, Zogona D, Wu T, et al. Applications, challenges and prospects of bionic nose in rapid perception of volatile organic compounds of food[J]. Food Chemistry, 2023: 135650.

[6] Qu C, Liu Z, Liu J, et al. Rapid determination of chemical concentration and odor concentration of paint-emitted pollutants using an electronic nose[J]. Building and Environment, 2023, 227: 109783.

[7] Li Y, Zhou W, Zu B, et al. Qualitative detection toward military and improvised explosive vapors by a facile TiO2 nanosheet-based chemiresistive sensor array[J]. Frontiers in Chemistry, 2020, 8: 29.

[8] Chen H, Huo D, Zhang J. Gas recognition in E-nose system: A review[J]. IEEE Transactions on Biomedical Circuits and Systems, 2022, 16(2): 169-184.

[9] Wu Z, Tian F, Covington J A, et al. Chemical selection for the calibration of general-purpose electronic noses based on Silhouette coefficients[J]. IEEE Transactions on Instrumentation and Measurement, 2022, 72: 1-9.

[10] Manzini I, Schild D, Di Natale C. Principles of odor coding in vertebrates and artificial chemosensory systems[J]. Physiological reviews, 2022, 102(1): 61-154.

[11] Ackels T, Erskine A, Dasgupta D, et al. Fast odour dynamics are encoded in the olfactory system and guide behaviour[J]. Nature, 2021, 593(7860): 558-563.

[12] Li G, Cleland T A. A coupled-oscillator model of olfactory bulb gamma oscillations[J]. PLoS computational biology, 2017, 13(11): e1005760.

[13] Viertel R, Borisyuk A. A Computational model of the mammalian external tufted cell[J]. Journal of theoretical biology, 2019, 462: 109-121.

[14] Kersen D E C, Tavoni G, Balasubramanian V. Connectivity and dynamics in the olfactory bulb[J]. PLoS computational biology, 2022, 18(2): e1009856.

[15] Park H, Sun Y, Jung S. Balanced Resistive Matrix Array for High-density Electrochemical Sensor Array[J]. IEEE Sensors Journal, 2023.

[16] Verhagen J V, Baker K L, Vasan G, et al. Odor encoding by signals in the olfactory bulb[J]. Journal of Neurophysiology, 2023, 129(2): 431-444.

[17] Sarkar S T, Bhondekar A P, Macaš M, et al. Towards biological plausibility of electronic noses: A spiking neural network based approach for tea odour classification[J]. Neural Networks, 2015, 71: 142-149.

[18] Wang T, Huang H M, Wang X X, et al. An artificial olfactory inference system based on memristive devices[J]. InfoMat, 2021, 3(7): 804-813.

[19] Vanarse A, Espinosa-Ramos J I, Osseiran A, et al. Application of a brain-inspired spiking neural network architecture to odor data classification[J]. Sensors, 2020, 20(10): 2756.

[20] Borthakur A, Cleland T A. A spike time-dependent online learning algorithm derived from biological olfaction[J]. Frontiers in neuroscience, 2019, 13: 656.

[21] Bohte S M, Kok J N, La Poutre H. Error-backpropagation in temporally encoded networks of spiking neurons[J]. Neurocomputing, 2002, 48(1-4): 17-37.

[22] Martinelli E, Polese D, Dini F, et al. An investigation on the role of spike latency in an artificial olfactory system[J]. Frontiers in neuroengineering, 2011, 4: 16.

[23] Dong Y, Zhao D, Li Y, et al. An unsupervised STDP-based spiking neural network inspired by biologically plausible learning rules and connections[J]. Neural Networks, 2023.

[24] Vergara A, Vembu S, Ayhan T, et al. Chemical gas sensor drift compensation using classifier ensembles[J]. Sensors and Actuators B: Chemical, 2012, 166: 320-329.